JOURNAL OF MATERIALS SCIENCE **34** (1999) 1341–1346

Study on intelligent humidity control materials: Water vapor adsorption properties of mesostructured silica derived from amorphous fumed silica

FUMIHIKO OHASHI*, MASAKI MAEDA, KEIICHI INUKAI, MASAYA SUZUKI, SHINJI TOMURA
Ceramic Technology Department, National Industrial Research Institute of Nagoya, AIST, MITI 1-1, Hirate, Kita, Nagoya, Aichi 462, Japan

The intelligent humidity control materials were synthesized using fumed silica and quaternary alkylammonium surfactant (decyl-, dodecyl-, tetradecyl- and hexadecyl-trimethylammonium chlorides) as a liquid-crystal template under hydrothermal conditions. X-ray diffraction and transmission electron micrographs indicate that a homogeneous hexagonal structure of SiO_2 was formed for those products. The mesostructured products had high B.E.T. surface areas between 960 and 1300 m^2/g, with uniform mesopore diameters of 2–4 nm. These physical quantities were controlled by varying the size of the organic template. Water vapor adsorption isotherms for these materials possess a sharp increase in adsorption when the relative water vapor pressure is at 40–60%. Over this range of pressures, the maximum amount of adsorbed water content is between 40 and 90%. These silicates have the potential to be effectively used as humidity control elements in construction materials.

1. Introduction

In recent years, our evolving and diverse lifestyles are demanding improved and more comfortable living environments in order to reduce allergic conditions and other technical problems. For instance, symptoms of atopy and asthma are caused by particles of tick and fungi, which grown well in high humidity. Alternatively, a build-up of static electricity occurs in low humidity, which can be harmful to electronic devices. Generally, in an attempt to control the relative humidity of our environment, air-conditioning equipment has been used; however, this method has the associated problem of high energy consumption. The used of organic, humidity-control materials in wall construction items have been utilized. However, it is well known that organic materials such as activated carbon tend to be flammable, weak and nondurable. In the case of inorganic compounds such as calcium chloride, silica-gel and zeolite, these materials exhibit poor water adsorption-desorption, with some being harmful to the human body.

Therefore, considering the above statements, there is a strong need to develop harmless inorganic materials which possess humidity control and high water adsorption capacity. Recently there has been a growing interest in the so-called mesoporous crystalline materials (MCM-41 type materials) because of their possible use as catalysts [1–4] and molecular sieves [5, 6]. Since the pore size can be designed from 2 to 10 nm using various sizes of an organic template, it seems reasonable that a porous silica having suitable humidity control properties can be produced.

In this study, the author used amorphous fumed silica and a quaternary alkylammonium template to produce mesostructured silica materials. These were created using a modified liquid-crystal templating method. The author investigated the effects of template size on material structure, particle and pore size distribution, specific surface area and water vapor adsorption. The results are discussed in the context of using these silicates as humidity control materials.

2. Experimental

2.1. Materials

Amorphous fumed silica was supplied from Nippon Aerosil Co. Ltd. (SiO_2, trade name Aerosil-300, >99.9 wt % purity). The organic template was comprised of the following quaternary alkyltrimethylammonium chlorides: using decyl- ($n = 10$), dodecyl- ($n = 12$), tetradecyl- ($n = 14$) and hexadecyl-trimethylammonium chloride ($n = 16$) ($C_nH_{2n+1}(CH_3)_3N^+ \cdot Cl^-$, 98% purity, Tokyo Chemical Industry Co. Ltd.). Sodium hydroxide used in these experiments was chemical reagent grade (NaOH, 96% purity, Wako Pure Chemical Co. Ltd.).

* Author to whom all correspondence should be addressed.

2.2. Preparation

Four mesoporous silicas were created by firstly preparing separate amorphous silica and template solutions. The amorphous fumed silica was dissolved into sodium hydroxide and stirred for 1 h. Separate aqueous suspensions (25 wt %) of decyl-, dodecyl-, tetradecyl- and hexadecyl-trimethylammonium chloride were then prepared. For each surfactant template, silica solution was added in the molar ratio of 1.00 : 0.17 : 53.00 : 0.50 ($SiO_2 : Na_2O : H_2O$: Surfactant) and then vigorously stirred for 1 h. These resulting sol mixtures were moved into separately 100 ml teflon-lined stainless steel autoclave vessels. All vessels were then put onto rollers in an electric oven at 30 rpm, 100 °C for 168 h for hydrothermal synthesis. After self-assemble reaction, the samples were quenched and washed with distilled water until they came to neutral pH. The resulting products were dried at 40 °C in an electric oven. In order to remove the organic template in the crystalline mesoporous silicas, the samples were heated in an electric furnace at 600 °C for 6 h under air current.

In this paper, these mesoporous materials are named "mesostructured silica-*n*", where *n* is the number of carbon atoms in the alkyl chain of the organic template.

2.3. Characterization

Powder X-ray diffraction analysis was carried out by a Geigerflex RAD-II-B diffractometer (Rigaku Co. Ltd., CN2155D5) using Ni-filtered CuK_α radiation at 20 mA and 30 kV. Morphology of the products was examined using a scanning electron microscopy (SEM) (Hitachi Co. Ltd., S-3200S). Transmission electron microscopy (TEM) was used to observe a lattice image with an accelerating voltage of 100 kV (JEOL Co. Ltd., JEM-200CX). Particle size distribution was determined by a centrifugal particle size analyzer (Shimadzu Co. Ltd., SA-CP3L). The Brunauer-Emmett-Teller (B.E.T.) surface area of the products was determined by means of nitrogen adsorption at liquid nitrogen temperature ($T = -195$ °C). Pore size distribution was measured by the Cranston-Inkley method using a nitrogen adsorption isotherm (Carlo Erba Instruments Co., Sorptomatic-1900). The isotherm of water vapor adsorption was determined by an adsorption isotherm analyzer (Tokyo Shikenki Manufacturing Co., EAM-01S) using approximately 0.3 g of product which had been under vaccum at 25 °C for one day. After complete evacuation, the relative humidity in the chamber was gradually increased from 10 to 90%. During this process, the increase in the samples weight represented the amount of adsorbed water vapor.

3. Results and discussion

3.1. X-ray diffraction

The X-ray diffraction profiles of the products in Fig. 1 show four well defined reflections which can be indexed with a very intense 100 diffraction peak and three weak 110, 200 and 210 peaks in a hexagonal symmetry. Table I summarizes the observed d_{100} basal spacing and the hexagonal unit-cell parameter, calculated using $a_0 = 2d_{100}/\sqrt{3}$. These results show d_{100} basal spacing, a measure of approximate pore diameter, increases as *n* increases (i.e., as the number of carbon atoms in the alkyl chain of the organic template increases). However, the relative intensity and the sharpness of the 100 reflection decreased with increasing *n*. Such low crystallinity is possibly explained by a lattice defect in the SiO_2 framework. Additionally, the participation of the pore wall thickness, which depends on the surfactant chain length, could also alter the crystallinity.

TABLE I d_{100}-spacing and hexagonal unit-cell parameter of the humidity control materials

Products	d_{100}-spacing (nm)	a_0 (nm)
Mesostructured Silica-10	3.02	3.49
Mesostructured Silica-12	3.27	3.78
Mesostructured Silica-14	3.59	4.15
Mesostructured Silica-16	3.62	4.18

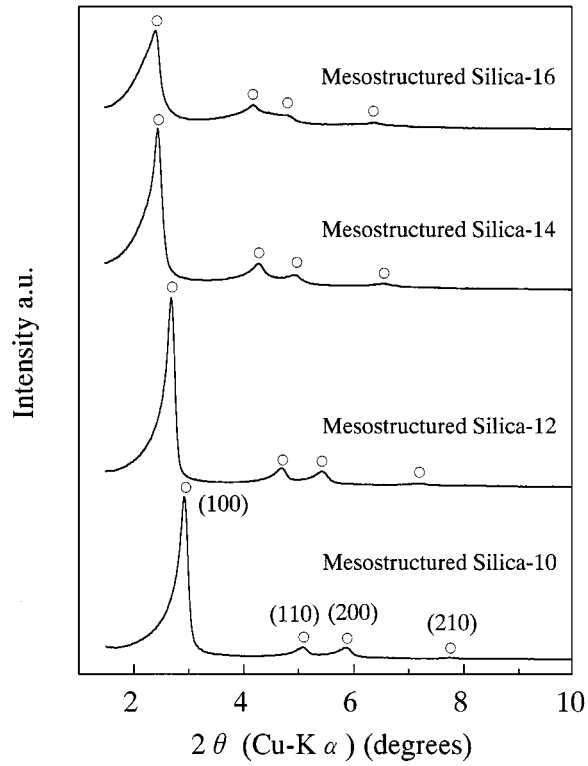

Figure 1 X-ray diffraction profiles of the humidity control materials. Relative intensity and crispness of reflections decrease as the surfactant chain increases in length.

3.2. SEM and TEM observation

Fig. 2 shows SEM and TEM photographs of the silica-dodecyltrimethylammonium complex ($n = 12$) after heat treatment. The SEM photograph indicates the presence of well-dispersed primary particles with diameters of approximately 0.2 to 0.3 μm. Regardless of the chain length of the organic surfactants, the particle size and morphology remained unchanged (Fig. 3). The TEM photograph reveals an indistinct hexagonal system and a well parallel channel corresponding to the side-on view of the tunnel-shaped pores. The diameter of the

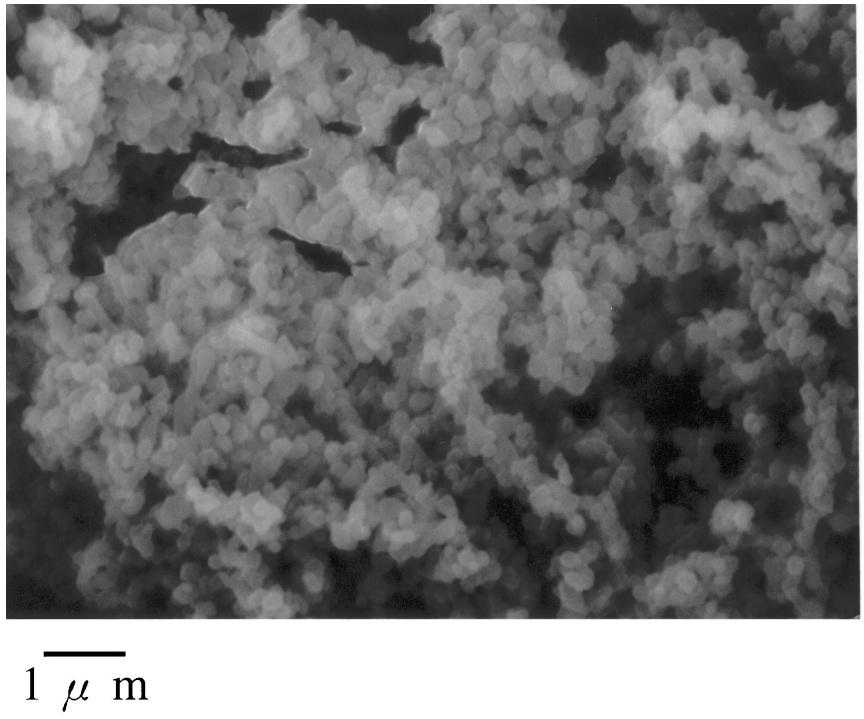

(A)

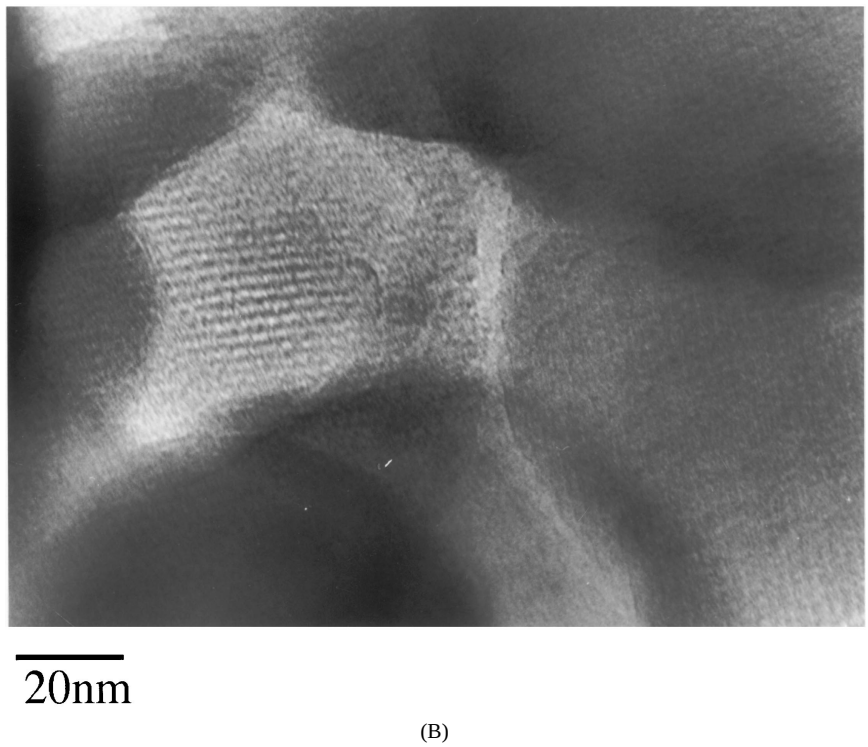

(B)

Figure 2 SEM (A) and TEM (B) photographs of the humidity control material ($n = 12$). (A): View of morphology of the primary particles of 0.2–0.3 μm in diameter. (B): TEM image showing the walls of the straight channel with particles of which unit-cell parameter is 3.78 nm.

regular array of channels is approximately 3 nm, which is in good agreement with the results from the X-ray diffraction analysis (Table I).

3.3. Particle size distribution

Particle size distribution of the silicas are illustrated in Fig. 3. The plot shows two peaks that correspond to 0.1–0.3 μm and to 10–20 μm. It is evident that the former peak coincides with the primary particle diameter observed in the SEM photograph, whereas the latter peak is likely to be associated with aggregates that form secondary particles.

3.4. Pore size distribution

Fig. 4 describes the pore size distribution of the products using the C.I. method. From these results, the pore size diameter increased from approximately 1.5 to 4 nm as the alkyltrimethylammonium chain length was increased. In addition, the range of the pore size distribution of the products was exceedingly narrow. These

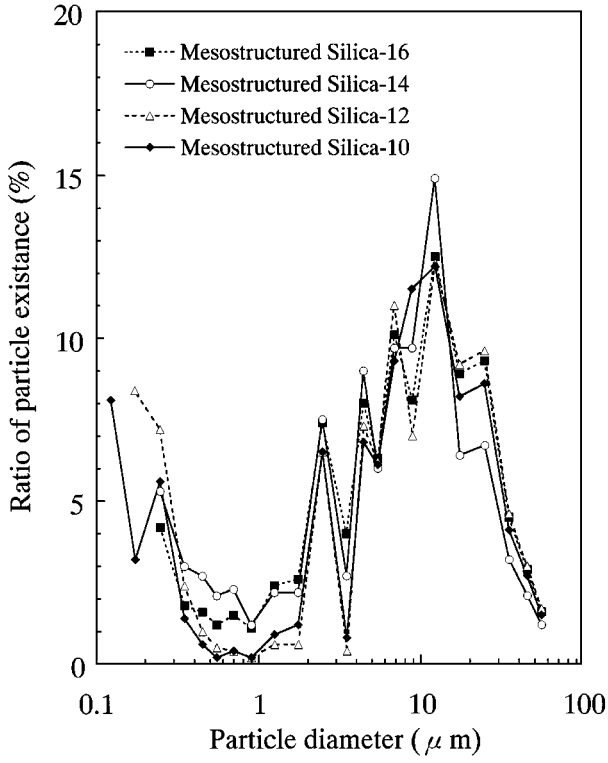

Figure 3 Particle size distribution of the humidity control materials, showing two distinct peaks near 0.1 and 10 μm.

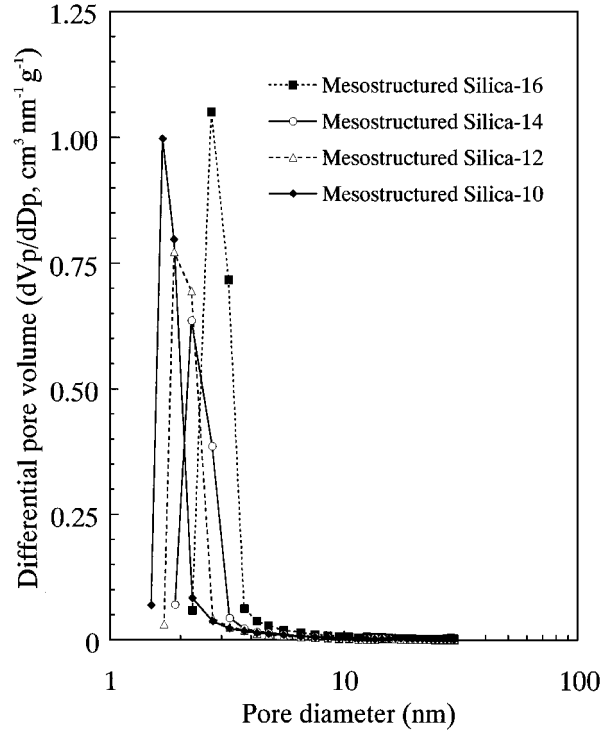

Figure 4 Pore size distribution of the humidity control materials. Pore diameter increased as template chain-length increased.

results indicate that pore size and distribution of such the homogeneous porous materials can be controlled and adjusted using various sizes of an organic template.

3.5. Specific surface area, total pore volume and average pore diameter

Table II lists the specific surface area (B.E.T. method), total pore volume and average pore diameter (C.I. method) of the products. All quantities tended to increase with increasing alkyl chain length. These remarkably large values of total pore volume are higher than those reported for pillared clays [7, 8] and commercialized zeolites [9]. The specific surface area ranged from 965 to 1344 m^2/g. The combination of having a high surface area and a narrow pore size distribution, indicates that most of the surface area is likely attributed to uniform arrangement of internal surfaces. In Table II, the values of average pore diameter are smaller than that of the unit-cell parameter (Table I). It is considered that the difference occurs because the hexagonal repeat distance of a_0 includes the SiO_2 pore wall thickness, there by increasing the average pore diameters.

TABLE II Characteristic data of the humidity control materials

Products	Specific surface area* (m^2/g)	Total pore volume** (ml/g)	Average pore diameter** (nm)
Mesostructured Silica-10	965	0.54	2.14
Mesostructured Silica-12	1233	0.62	2.36
Mesostructured Silica-14	1137	0.65	2.70
Mesostructured Silica-16	1344	1.10	3.20

*: B.E.T. adsorption method using N_2 gas.
**: Cranston-Inkley method.

3.6. Water vapor adsorption isotherm

The water vapor adsorption isotherms are shown in Fig. 5. A commercialized humidity control material

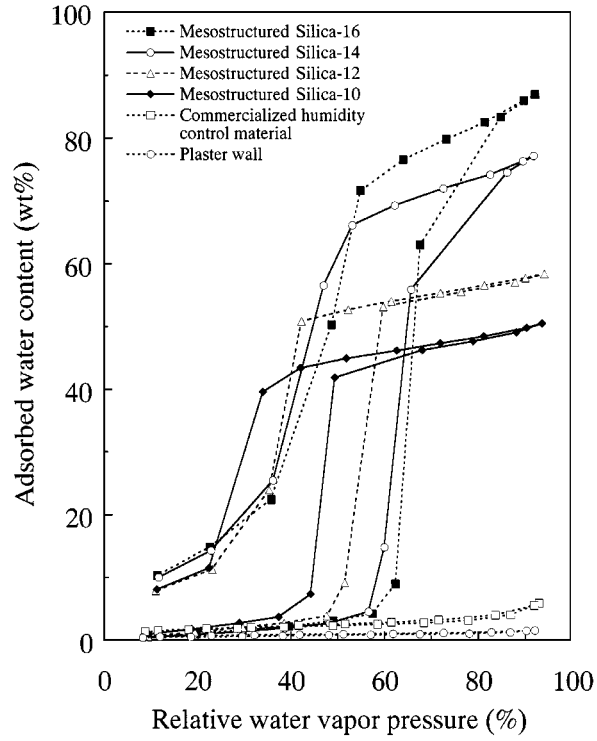

Figure 5 Water vapor adsorption-desorption isotherms of the humidity control materials plotted with references.

(trade name MUSELITE, Asahi Glass Co., Ltd.) and a plaster wall (main constituent: calcite, lime) are plotted for comparison. The synthesized products exhibited quite distinct adsorption-desorption curve that indicate an inflection characteristic of capillary condensation within opened pores. The relative pressure at which this inflection occurred increased with increasing pore size. The relation between relative-humidity (P/P_0) and pore diameter (d) is estimated using Kelvin's capillary condensation equation as follows,

$$d = -(4\gamma M \cos\theta)/(\rho RT \ln(P/P_0))$$

where γ, M, θ, and ρ are the surface tension, molecular weight, contact angle and density of the liquid, R is the gas constant and T is the absolute temperature [10, 11]. Pore filling and emptying with water vapor occurred sharply over relative pressures of 40 to 60%, which correspond to approximate pore diameters of 2.1 to 4.2 nm calculated from Kelvin's equation. These values are in good agreement with the results obtained from the nitrogen adsorption method. Although Komarneni *et al.* also analyzed the water vapor adsorption-desorption properties of the mesoporous materials, they did not account for the control of the pore size distribution [12]. The primary consideration in setting up any porous materials for humidity control materials should be the control of pore sizes. By controlling of the pore diameter in the materials, the amount of adsorbed water increased vertically and steeply on suitable relative water vapor pressure.

The total amount of adsorbed water was determined by the specific surface area and the pore volume. These quantities control the effective surface available for water vapor adsorption. From these results, in order to obtain a large amount of water adsorption and a high humidity-control ability, it is necessary to control the pore diameter, the B.E.T. surface area and the pore volume. Moreover, the humidity control efficiency is better for the synthesized products than for the reference materials. However, the synthesized materials have an associated hysteresis loop. This phenomenon can possibly be due to the difference between condensation and evaporation of the liquid water meniscus, and/or some of chemically adsorbed water molecules connected to the silicon atoms as a silanol group [13]. The water vapor adsorption isotherms for the repeated cycles are shown in Fig. 6. Although the total amount of adsorbed water was slightly decreased by the repeated cycles using water vapor, such decreases did not influence the humidity control abilities in practice. The narrower hysteresis loops for the repeated cycles of the water isotherms could be explained by the smaller contact angle due to the rehydration on the internal surface. The relative pressure at the sudden increase shifted to lower values after repeated adsorption isotherms. This suggests a decrease of the pore diameter for the chemically adsorbed water molecules after the first few cycles. By controlling the shapes of the hysteresis loops between 40 and 70% relative humidity, which is the preferable range for the living environment, it is possible to prepare more functional materials with desired humidity control abilities.

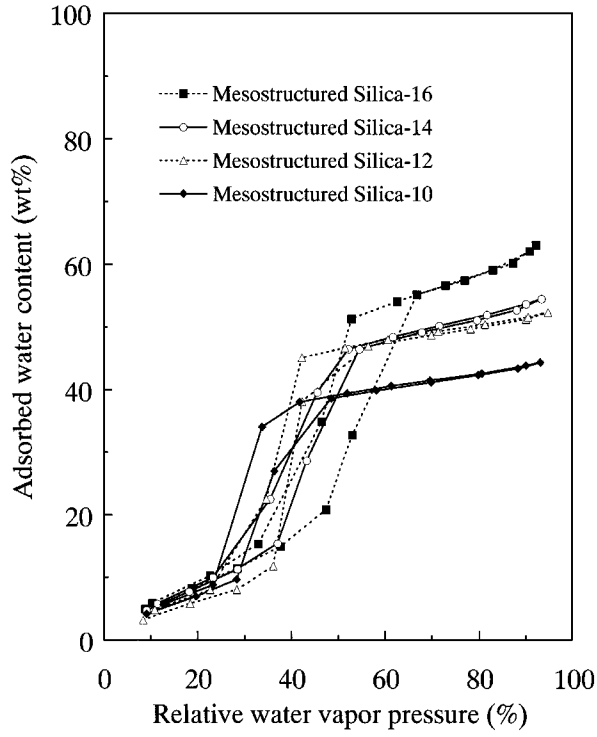

Figure 6 Water vapor adsorption-desorption isotherms of the humidity control materials for the repeated cycles.

4. Conclusions

The intelligent humidity control materials were synthesized by a hydrothermal reaction of fumed silica with alkyltrimethylammonium surfactant as the liquid-crystal template. Powder X-ray diffraction and TEM observations revealed that periodic hexagonal mesostructured silica was formed after calcining the hydrothermal product. The silicas have an uniform mesoporous architecture in which the pore diameter was dependent on the template chain-length. In the instance of water vapor adsorption-desorption behavior, the products showed higher maximum adsorption and the isotherm curves increased at a more suitable relative humidity than those of commercialized humidity control materials. Some additional properties will be examined for practical application in the future.

Acknowledgements

A part of this study has been supported by the "Government and Private Joint Research Project, AIST, MITI".

References

1. R. BRUCH, N.CRUISE, D.GLEESON and S. C. TSANG, *J. Chem. Soc., Chem. Commun.* **8** (1996) 951.
2. T. MASCHMEYER, F. REY, G. SANKAR and J. M. THOMAS, *Nature* **378** (1995) 159.
3. W. ZHANG, J. WANG, P. T. TANEV and T. J. PINNAVAIA, *J. Chem. Soc., Chem. Commun.* **8** (1996) 979.
4. D. R. C. HUYBRECHTS, L. DE BRUYCKER and P. A. JACOBS, *Nature* **345** (1990) 240.
5. M. E. DAVIS and R. F. LOBO, *Chem. Mater.* **4** (1992) 756.
6. J. S. BECK, J. C. VARTULI, W. J. ROTH, M. E. LEONOWICZ, C. T. KRESGE, K. D. SCHMITT, C. T-W. CHU, D. H. OLSON, E. W. SHEPPARD, S. B. MCCULLEN, J. B. HIGGINS and J. L. SCHLENKER, *J. Amer. Chem. Soc.* **114** (1992) 10834.

7. M. L. OCCELLI, S. D. LANDAU and T. J. PINNAVAIA, *J. Catal*. **90** (1984) 256.
8. T. J. PINNAVAIA, *Science* **220** (1983) 365.
9. J. M. THOMAS and D. E. W. VAUGHAN, *J. Phys. Chem. Solids* **50** (1989) 444.
10. L. R. FISHER and J. N. ISRAELACHVILI, *J. Colloid Interface Sci*. **80** (1981) 528.
11. J. C. MELROSE, *Langmuir* **5** (1989) 290.
12. S. KOMARNENI, R. PIDUGU and V. C. MENON, *J. Porous Mater*. **3** (1996) 99.
13. R. K. ILER, "The Chemistry of Silica" (John Wiley & Sons, New York, 1979) p. 622.

Received 30 June 1997
and accepted 8 October 1998